

3-5 Total Radiated Power of Radio Transmitters Measured in a Reverberation Chamber

HARIMA Katsushige, SUGIYAMA Tsutomu, YAMANAKA Yukio,
and SHINOZUKA Takashi

A random electromagnetic field is created in a reverberation chamber by moving mechanical stirrers to vary the boundary condition. The received E-field strength caused by moving the stirrer is Rayleigh distributed and the field distribution is statistically uniform in an ideal reverberation chamber. The total radiated power of the EUT is obtained by the substitution method from the average or median value of the E-field when the receiving antenna is placed so as to avoid the influence of the direct wave from the EUT. However, using the substitution method requires a great deal of time to measure the averaged received level for a broadband radiated source. The dimensions of the chamber and the structure of the stirrers affect the field uniformity in an actual chamber. The statistical characteristics of the spatial E-field distribution in a reverberation chamber are described, along with an efficient technique for measuring total radiated power of broadband radiation sources and the statistical technique using a 63.2% value of the cumulative distribution that can reduce the influence of the direct wave.

Keywords

Reverberation chamber, Total radiated power, Rayleigh distribution, Rice distribution, Multi path, Stirrer

1 Introduction

Designed to generate a statistically uniform electric field by varying boundary conditions with stirrers provided in a shielded enclosure[1], the reverberation chamber is used for EMC measurements, including radiated emission and immunity measurements[2][3]. This chamber is also an effective means of measuring the radiated power of radio transmitters with built-in antennas.

Measuring radiated power with a reverberation chamber is accomplished by placing the equipment under test (EUT) within the test volume of the chamber and estimating the total radiated power from the mean, median, or maximum value of received power obtained by rotating the stirrer. If the direct wave component is included in the received power, it

causes measurement errors. On the other hand, the uniformity of the spatial electric field distribution in an ideal reverberation chamber can be theoretically estimated from the probability density function of its distribution[4][6]. However, uniformity in an actual chamber is affected by the dimensions of the chamber and the structure of the stirrers[5][6].

Meanwhile, spurious measurement based on regulations governing unwanted emissions and radiated power measurement of ultra wideband (UWB) devices using short pulse signals requires measurement over a wide frequency band. However, using conventional measurement methods requires a great deal of measurement time for a broadband radiated source.

This paper will first present the results of comparison between theoretical and measured

values for spatial uniformity of electric field distribution in a reverberation chamber [6], and will then introduce two methods: the improved mode-stirred method [7][8], capable of measuring radiated power of broadband radiation sources in a short period of time; and the statistical technique [9], a measurement method that can reduce direct wave effects. The latter method applies a 63.2% value of the cumulative distribution function (CDF) of received power.

2 Statistical characteristics of the electric field

2.1 Probability density function

The electric field in a reverberation chamber varies considerably with changes in the boundary condition as a result of the movement of the stirrer. When the reverberation chamber is large relative to the wavelength, that is, when a sufficient number of resonant modes within the chamber exist, the electric field at a given position in the chamber is the sum of multipath plane waves with random phases caused by moving of the stirrers.

Generally, the total number of resonant modes (n) occurring in a rectangular shielded enclosure is given approximately by the *Weyl* formula [1]:

$$n \cong \frac{8\pi abc}{3\lambda^3} \quad (1)$$

where a , b , and c are the dimensions of the chamber and λ is the wavelength.

The electric field vector E at a given point in the reverberation chamber can be expressed by the following formulas using three rectangular components, each of which consists of a real and imaginary part, that is, six parameters in total:

$$\mathbf{E} = E_x + E_y + E_z \quad (2)$$

$$E_{x,y,z} = \text{Re}(E_{x,y,z}) + i \text{Im}(E_{x,y,z}) \quad (3)$$

As the stirrer moves, an extremely large number of multipath waves are generated. Hence, each real and imaginary part of the

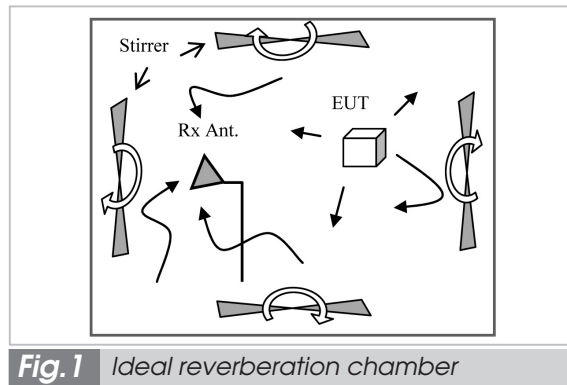


Fig. 1 Ideal reverberation chamber

rectangular components of the electric field is normally distributed by the central limit theorem. Since these real and imaginary parts are not correlated, they are independent random variables. If a reverberation chamber is ideal, the mean value and the mean square value of the real and imaginary part of the rectangular component are given respectively by [10]:

$$\langle \text{Re}(\mathbf{E}_{x,y,z}) \rangle = \langle \text{Im}(\mathbf{E}_{x,y,z}) \rangle = 0 \quad (4)$$

$$\begin{aligned} \langle \text{Re}(\mathbf{E}_{x,y,z})^2 \rangle &= \langle \text{Im}(\mathbf{E}_{x,y,z})^2 \rangle \\ &= E_0^2 / 6 \equiv \sigma^2 \end{aligned} \quad (5)$$

where E_0^2 is the mean square of the magnitude of the electric field E and σ^2 is the variance.

Therefore, six parameters of the electric field are independent random variables and each parameter is normally distributed with zero mean and variance σ^2 . The sum of the square values of the six parameters, i.e. the squared magnitude of the resultant field, is the chi-square (χ^2) distributed with six degrees of freedom. Similarly, the root value of the chi-square distribution, i.e., the magnitude of the resultant field, is chi distributed with six degrees of freedom. The probability density functions of these distributions are given respectively by [10][11]

$$f(|\mathbf{E}|^2) = \frac{|\mathbf{E}|^4}{16\sigma^6} \exp\left(-\frac{|\mathbf{E}|^2}{2\sigma^2}\right) \quad (6)$$

$$f(|\mathbf{E}|) = \frac{|\mathbf{E}|^5}{8\sigma^6} \exp\left(-\frac{|\mathbf{E}|^2}{2\sigma^2}\right) \quad (7)$$

Usually, the E-field in the chamber is measured using a linear polarized antenna. The

received data corresponds to one rectangular component with two parameters of the field and is therefore the chi-distributed with two degrees of freedom. The probability and cumulative density function of this chi distribution, which has the same characteristic of a Rayleigh distribution, are given respectively by [10][11]

$$f\left(\left|E_{x,y,z}\right|\right)=\frac{\left|E_{x,y,z}\right|}{\sigma^2}\exp\left(-\frac{\left|E_{x,y,z}\right|^2}{2\sigma^2}\right) \quad (8)$$

$$F\left(\left|E_{x,y,z}\right|\right)=1-\exp\left(-\frac{\left|E_{x,y,z}\right|^2}{2\sigma^2}\right) \quad (9)$$

2.2 Uniformity of spatial electric field distribution

The spatial uniformity of the electric field distribution in a reverberation chamber is affected by the number of independent stirrer positions, i.e., the number of positions to which the stirrers move that produces uncorrelated fields in the chamber. If an ideal reverberation chamber is used, the received E-field strength at a given measurement point in the chamber caused by moving the stirrers is Rayleigh distributed, as described in the previous paragraph. The spatial E-field obtained by moving the measurement point at a fixed stirrer position ($N = 1$) is also Rayleigh distributed.

The mean and maximum electric field distributions obtained by N stirrer positions was found by random sampling of the N data from the Rayleigh distribution. Figure 2 shows the probability density functions (PDF) of the mean and maximum electric field distributions calculated from random samplings.

The probability density function of the maximum electric field distribution can also be estimated by applying the extreme value theory [12]. That is, taking the maximum value $x(N)$ of the N independent samples to be the random variable, the cumulative density function $F_N(x)$ and the probability density function $f_N(x)$ of the maximum value are represented by

$$F_N(x) = F(x)^N \quad (10)$$

$$f_N(x) = N \cdot F(x)^{N-1} \cdot f(x) \quad (11)$$

Figure 2(b) shows the calculation results for the probability density function of the maximum electric field distribution determined from formulas (8), (9), and (11). The theoretical values calculated by the extreme value theory agree with those determined by random sampling.

The uniformity of the mean, median, and maximum E-field distribution was derived by the probability density functions of those distributions shown in Fig. 2. The standard deviation of those distributions as a function of the number of stirrer positions is shown in Fig. 3. The uniformity of the distributions was improved rapidly and then slowly by increasing the number of stirrer positions. The uniformity of the maximum distribution was worse than that of the averaged and median distributions at the same number of stirrer positions. For example, the number of stirrer positions required to obtain the standard deviation of the mean, median, and maximum distributions

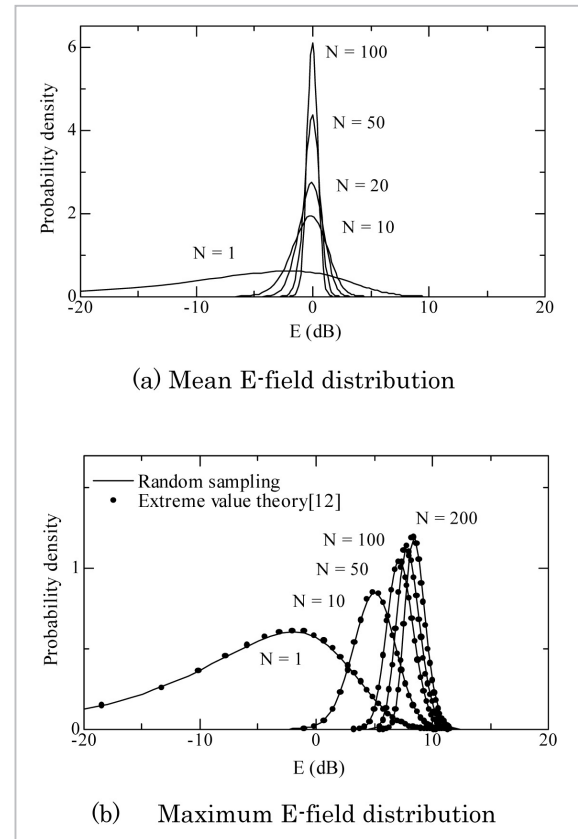


Fig.2 Probability density function of the mean and maximum E-field distributions as a function of the number of stirrer positions

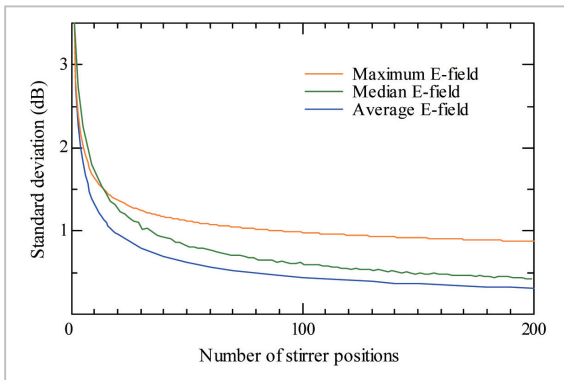


Fig.3 Uniformity of mean, median, and maximum E-field distribution as a function of the number of stirrer positions

within 1 dB was more than 19, 34, and 92 positions, respectively.

As described above, assuming an ideal reverberation chamber, the uniformity of the electric field distribution can be obtained theoretically using the probability density function of that distribution, which is a function of the number of stirrer positions. However, uniformity in an actual chamber is affected by the operating frequency and the structure of the stirrers. Theoretical and measured values were compared to assess these effects on uniformity.

Figure 4 shows two reverberation chambers used in measurement; these differed in size, stirrer structure, and number of stirrers equipped. The electric field distribution was measured over frequencies from 200 MHz to 3 GHz at 125 measurement points partitioned by grids of $5 \times 5 \times 5$ at intervals of 25 cm by setting up $1 \text{ m} \times 1 \text{ m} \times 1 \text{ m}$ measurement vol-

umes in these reverberation chambers.

Figure 5 shows a comparison of uniformity between measured and theoretical values for the mean electric field distribution. Uniformity is in good agreement with the theoretical value when the dimensions of a chamber are large compared to the wavelength at the operating frequency, that is, when a sufficient number of resonant modes exist. The experimental results show also that the spatial field uniformity depends on the frequency and is not greatly improved at lower operating frequencies with an insufficient number of resonant modes. Moreover, the figure indicates that uniformity is affected by the stirrer structure.

3 Radiated power measurement method

This chapter presents two radiated power measurement methods reviewed using a reverberation chamber. Section 3.1 will introduce efficient methods of measuring radiated power from a broadband radiation source, and Section 3.2 will discuss statistical techniques ensuring the reduction of direct wave effects.

3.1 Improved mode-stirred method

Two standard measurement methods, the mode-stirred and mode-tuned method, are available for measuring radiated power using a reverberation chamber [2].

The mode-stirred method continuously rotates the stirrer and measures the variation in

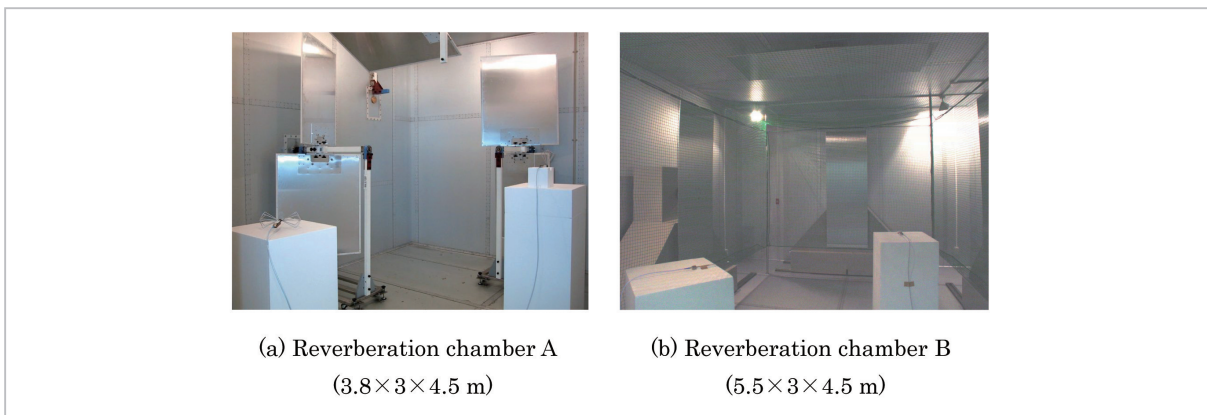


Fig.4 Reverberation chamber

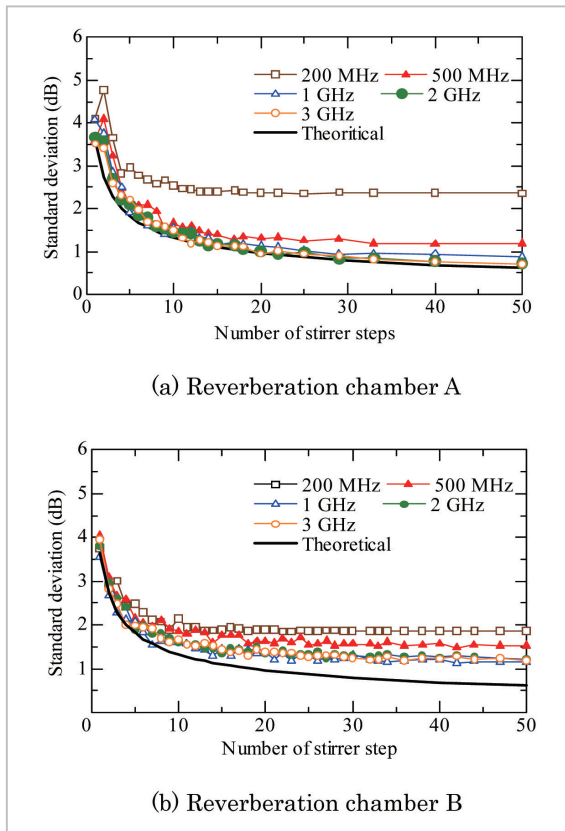


Fig.5 Uniformity of mean E-field distribution

the received level over the period of one rotation of the stirrer at discrete frequencies, thus requiring a significant amount of time to measure the received level over a wide frequency span. In the mode-tuned method, the received level is measured at a desired full frequency span at each stirrer's position as the stirrers are moved in discrete steps. Although effective for measurement over a wide frequency span, this method requires a number of steps to rotate the stirrer, entailing difficulty in controlling the stirrer's drive system. We proposed an improved method capable of measuring radiated power from a broadband radiation source in a short period of time (i.e., within several minutes) and experimentally verified the efficacy of the proposed method [7][8].

Transmitting and receiving antennas are placed in a reverberation chamber and connected to a spectrum analyzer and signal generator, as shown in Fig. 6. Input power $P_{in}(f)$ is applied to the transmitting antenna and then

the received power $P_r(f)$ of the receiving antenna and the reflected power $P_{ref}(f)$ from the transmitting antenna are measured for a period of one rotation while continuously rotating the stirrer. The averaged net input power $P_{net}(f)$ to the transmitting antenna during the stirrer rotation is

$$P_{net}(f) = P_{in}(f) - P_{ref}(f) \quad (12)$$

The total radiated power $P_{Total}(f)$ of the EUT is obtained by the substitution method, i.e., the EUT is replaced at the same location with the transmitting antenna, and the two averaged received powers $P_r(f)$ and $P_{eut}(f)$ during the stirrer rotation are compared. That is,

$$P_{Total}(f) = P_{eut}(f) \cdot \frac{P_{net}(f)}{P_r(f)} \quad (13)$$

The frequency span of the spectrum analyzer should be set to as wide a range as possible, and the analyzer's sweep speed should be set sufficiently high relative to the stirrer's rotational speed so as to provide a number of samples over a period of one rotation of the stirrer. The received power obtained over one rotation is averaged with the watt value using the sample detection mode of the spectrum analyzer.

3.1.1 Experimental results and discussion

Radiated power was measured by the improved mode-stirred method using a reverberation chamber. Double-ridged guide horn

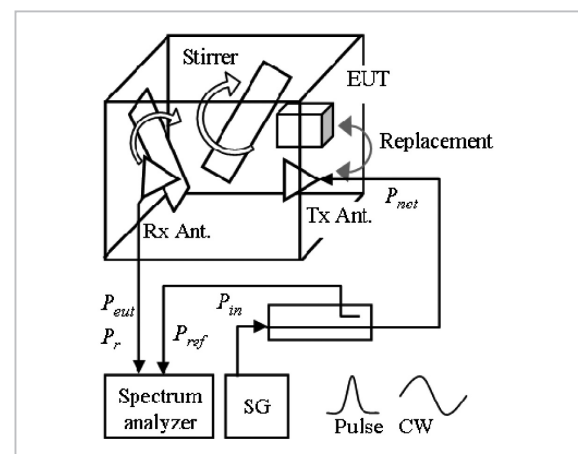


Fig.6 Experimental setup

antennas were used as transmitting and receiving antennas and connected to the spectrum analyzer. The transmitting antenna was placed so as to prevent illuminating the test volume directly and thus to avoid the influence of a direct wave. As the EUT, a comb generator was used to generate pulse signals with a pulse width of 84 ps and pulse period of 10 ns. This comb generator was equipped with a double-ridged guide horn antenna.

The radiated power was measured over a frequency range of 1 to 18 GHz by rotating three stirrers at different speeds (1, 2, and 3 rpm). The received power was measured over 120 sweeps during one rotation of stirrers using the spectrum analyzer at the frequency sweep time of 390 ms at intervals of 4 GHz span (20001 points). The total radiated power was determined from the average received power of the data obtained from the 120 sweeps.

Figure 7 shows the output shape of the pulse signal of the comb generator and the shape of the received signal in the reverberation chamber. The figure indicates that the pulse signal with short duration is distorted due to the high-Q factor of the chamber. When a reverberation chamber is used for the total radiated power of pulse signals, the measurement results applied by continuous wave (CW) substitution may be possibly affected by a distortion of the pulse signal, depending on the pulse duration, due to the chamber's high-Q factor. Hence, a pulse signal similar to the EUT's output pulse was substituted for a continuous wave, and the results were compared

with those obtained by the CW substitution.

Figure 8 shows the measurement results for radiated power of the comb generator. The results obtained by the improved mode-stirred method agree well with those obtained by the mode-turned method, thus confirming the efficacy of the improved method. Moreover, the measurements time of 5 minutes was obtained by using the improved method, that is, this indicates the efficacy of measuring the radiated power in a short period of time for a broadband radiation source. However, the radiated power measured by applying the CW substitution was shifted by 3–5 dB more than the output level of the comb generator, while that for the pulse substitution agreed with the output level. These results suggest that the pulse substitution using a pulse waveform similar to the EUT's pulse signal is effective in measuring the radiated power of short pulse signals.

3.2 Statistical estimation method

3.2.1 Principle

When a radio transmitter and receiving antenna are arranged in a reverberation chamber, a direct wave from the transmitter and reflected waves with random phases created by rotating stirrers arrive at the receiving antenna. The probability density function $p(r)$ of the received power r , i.e., the mixed waves combining the direct wave and multipath waves, is given by the following formula, and the received power is Rice distributed [13].

$$p(r) = \frac{r}{\sigma^2} \exp\left(-\frac{r^2 + A^2}{2\sigma^2}\right) I_0\left(\frac{A r}{\sigma^2}\right) \quad (14)$$

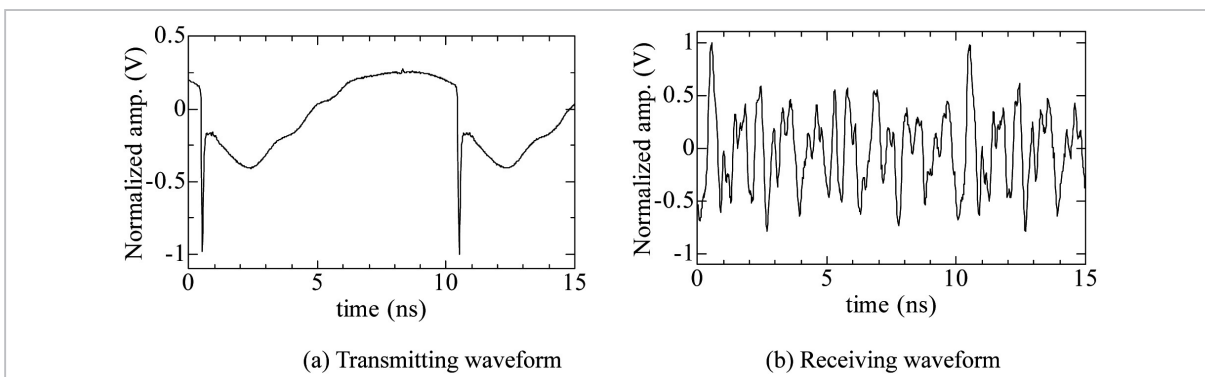


Fig.7 Pulse signal of comb generator

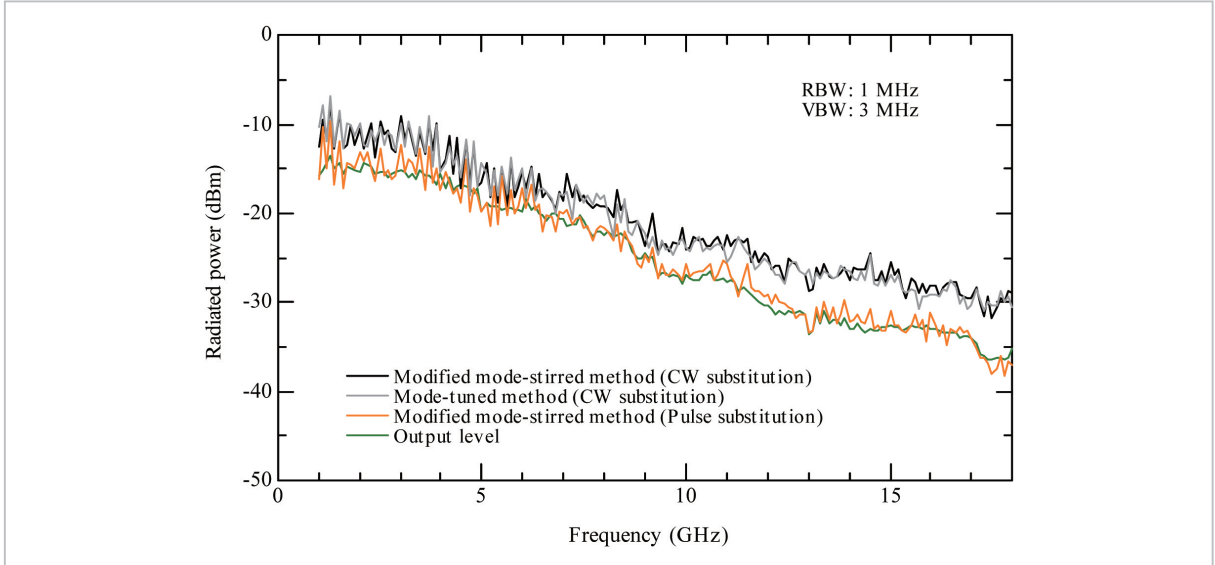


Fig.8 Experimental results

where σ^2 is the power corresponding to the multipath waves, $A^2/2$ is the power corresponding to the direct wave, and I_0 is a 0th-order modified Bessel function.

Defining the ratio of direct and multipath wave power as ρ and normalizing r by the square root of the sum of direct and multipath wave power, formula (14) can be rewritten as follows:

$$p(R) = 2(1+\rho)R \cdot \exp\left\{-\left[\rho + (1+\rho)R^2\right]\right\} \cdot I_0\left[2R\sqrt{\rho(1+\rho)}\right] \quad (15)$$

where

$$\rho = \frac{A^2/2}{\sigma^2} \quad (16)$$

$$R = \frac{r/\sqrt{2}}{\sqrt{A^2/2 + \sigma^2}} \quad (17)$$

Figure 9 shows the cumulative distribution function (CDF) $F(R)$ derived by integrating R in the Eq. (15). When $\rho \rightarrow \infty$, $F(R) = U(R-1)$, where U is the step function. When $\rho = 0$, $F(R) = 1 - \exp(-R^2)$, thus reflecting the same characteristics as those of the Rayleigh distribution. These curves intersect at a CDF of $R = 1$, namely, at $0.632 (= F(1))$. The intersection point shifts somewhat with respect to r between the two curves, but it will be apparent from Fig. 9 that the degree of slippage is never

more than 0.5 dB when the CDF is 63.2%. In other words, the 63.2% value of CDF of the normalized envelope is practically constant for any value of ρ .

When a transmitting antenna T and receiving antenna R are placed in a reverberation chamber as shown in Fig. 10, the radiated power P_T is given by

$$P_T = P_F \cdot (1 - |\Gamma_T|^2) \quad (18)$$

where P_F is the input power to the antenna T and Γ_T is the reflection coefficient of antenna T.

Assuming that the 63.2% value of CDF of the received signal is P_{TR63} , the chamber loss

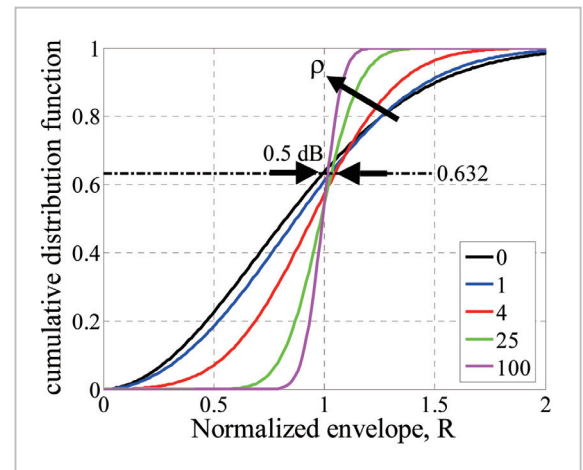


Fig.9 Cumulative distribution function of rice distribution

LC can be defined by

$$L_C = \frac{P_T}{P_{TR63}} \quad (19)$$

When the transmitting antenna T is replaced by EUT, the above formula can be rewritten as follows

$$\frac{P_{EUT}}{P_T} = \frac{P_{EUTR63}}{P_{TR63}} \quad (20)$$

Hence,

$$P_{EUT} = P_{EUTR63} \cdot L_C \quad (21)$$

where P_{EUT} is the radiated power of EUT and P_{EUTR63} is 63.2% of the value of CDF of the received signal.

Therefore, the radiated power of EUT can be estimated from the chamber loss L_C and the 63.2% value of CDF of the received signal. This technique ensures high accuracy in measurement even under the condition in which a direct wave exists [9].

3.2.2 Example of measuring radiated power of 2.45 GHz radio transmitter

In the measurement of total radiated power of the radio transmitters by the substitution method, the substitute antenna can be placed anywhere in an ideal reverberation chamber. However, the uniformity of the electric field in an actual chamber is affected by the operating frequency and by stirrer structure. As a result, the chamber loss varies depending on the antenna position. For example, if the EUT has an unknown radiation source, as with wireless LAN equipment built into a laptop PC, the

measured value will vary depending on the position of the substitute antenna. For this reason, effects of the substitute antenna location were reviewed using a “dummy” laptop PC with a built-in 2.45 GHz signal generator. The dummy laptop PC consists of an actual laptop PC with components such as motherboard and hard disk drive, etc. removed. In the bare chassis is installed a 2.45 GHz transmitter. An antenna for a PCMCIA wireless LAN card was used as the transmitting antenna.

The radiated power of the dummy laptop PC was estimated using the 63.2% value of CDF of the received signal by moving the laptop PC in four directions, spaced 90 degrees apart in the horizontal plane [14]. The chamber loss was determined as the mean of losses measured by the substitute antenna at five points in the vicinity of the antenna of laptop PC and at six points in the vicinity of the PC enclosure.

Figure 12 shows the measurement results. The true value of radiated power was assessed by correcting the measured value obtained by directly connecting a power meter to the antenna cable, i.e., antenna input power, and the measured value of the reflection coefficient (variation width: 0.3 dB) of the antenna in the reverberation chamber.

When the substitute antenna was placed in the vicinity of the center of the PC enclosure (marked “O”) and the antenna of EUT (marked “◇”), the difference between the true value and the measured was within 1.5 dB and 0.5 dB, respectively. For the mean of the radiated power values measured in the four different directions, however, when that of the center of the PC enclosure, the difference between the true value and the measured was within 0.6 dB, and when that of the antenna of EUT, the measured value was agreed with the true value.

4 Conclusions

We experimentally and theoretically reviewed the statistical characteristics of the electric field distribution in a reverberation

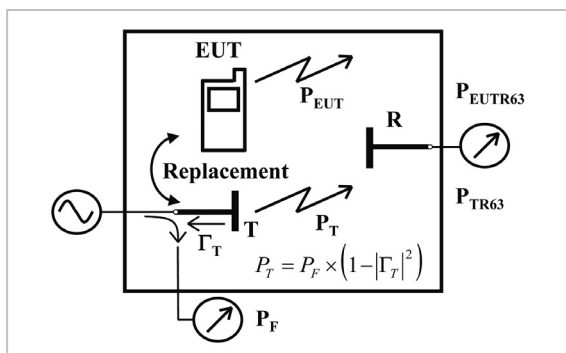


Fig. 10 Chamber loss and radiated power measurement

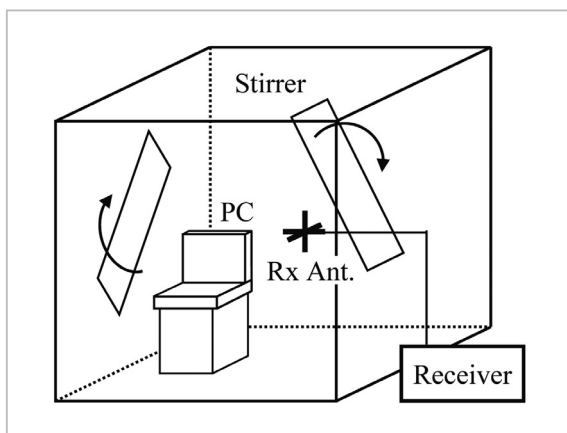


Fig. 11 Setup for radiated power measurement

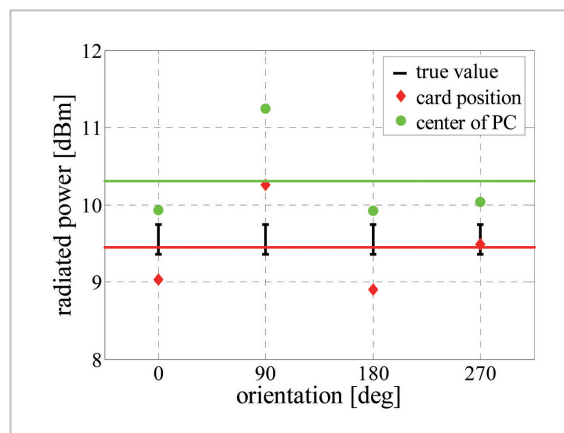


Fig. 12 Measured result of radiated power from dummy laptop PC

chamber and evaluated the effects of stirrers on the spatial uniformity of the electric field distribution.

The improved mode-stirrers method was proposed for the total radiated power measurement of broadband radiation sources and its efficacy was confirmed. Experimental results demonstrated that the measured results through application of the CW substitution include errors, while the pulse substitution is effective in measuring the radiated power of short pulse signals.

Further, we proposed a statistical technique to estimate the radiated power using a 63.2% value of the cumulative distribution for reducing the influence of the direct wave. Through results measured by this method for a 2.45 GHz radio transmitter, it was demonstrated that radiated power can be very accurately estimated by precisely matching the position

of the EUT's radiation source with the position of the substitute antenna or by using the mean value at positions in the vicinity of the radiation source.

Future work is needed to evaluate the effects of pulse width and to investigate a method for spurious measurements, as well as a method of measuring radiated power for large EUT such as floor-standing equipment.

Acknowledgements

We would like to express our deep appreciation to Mr. Kyoichi Nakajima and Mr. Tomoyuki Nojima of the Telecom Engineering Center for generously lending their “dummy” laptop PC (with 2.5 GHz radio transmitter) for verification of the statistical estimation method.

References

- 1 M. L. Crawford and G. H. Koepke, “Design, evaluation, and use of a reverberation chamber for performing electromagnetic susceptibility/vulnerability measurements”, National Bureau of Standards Technical Note 1092, Apr. 1986.
- 2 IEC 61000-4-21, “Testing and measurement techniques - reverberation chamber test methods”, 2003.
- 3 CISPR Publication 16-1, “Reverberation chamber for total radiated power measurement”, 1996.
- 4 M. O. Hatfield, “A calibration procedure for reverberation chambers”, Proc. 2000 IEEE International Symposium on EMC, pp.621-626, Washington D. C., USA, Aug. 2000.
- 5 K. Harima and Y. Yamanaka, “Evaluation of electric-field uniformity in a reverberation chamber for radiated immunity testing”, IEICE Trans. Commun., Vol.E84-B, No.9, pp.2618-2621, Sep. 2001.

-
- 6 K. Harima, "Statistical Characteristics of E-Field Distribution in a Reverberation Chamber", IEICE Trans. Commun, Vol. E88-B, No. 8, pp. 3127-3132, Aug. 2005.
 - 7 K. Harima and Y. Yamanaka, "Determining Total Radiated Power for Short Pulse Signals by Using a Reverberation Chamber", Proc. EMC Europe Workshop 2005, pp. 77-79, Rome, Italy, Sep. 2005.
 - 8 K. Harima, "Radiated Emission Measurement of Small EUT by Using a Reverberation Chamber", Proc. 2003 IEEE EMC Symposium, pp. 471-474, Istanbul, TURKEY, May 2003.
 - 9 T. Sugiyama, T. Shinozuka, and K. Iwasaki, "Estimation of Radiated Power of Radio Transmitters Using a Reverberation Chamber", IEICE Trans. Commun., Vol. E88-B, No. 8, pp. 3158-3163, Aug. 2005.
 - 10 G. Kostas and B. Boverie, "Statistical model for a mode-stirred chamber", IEEE Trans. Electromagn. Compat., Vol.33, No.4, pp.366-370, Nov. 1991.
 - 11 D. A. Hill, "Plane wave integral representation for fields in reverberation chambers", IEEE Trans. Electromagn. Compat., Vol.40, No.3, pp.209-217, Aug. 1998.
 - 12 T. H. Lehman and G. J. Freyer, "Characterization of the maximum test level in a reverberation chamber", Proc. 1997 IEEE International Symposium on EMC, pp.44-47, Austin, USA, Aug. 1997.
 - 13 S. O. Rice, "Statistical properties of a sine wave plus random noise", Bell Syst. Tech. J., Vol. 27, pp.109-157, Jan. 1948.
 - 14 M. Uchino, O. Tagiri, and T. Shinozuka, "Real-Time Measurement of Noise Statistics", IEEE Trans. Electromagn. Compat., Vol.43, No.4, pp.629-636, Nov. 2001.

HARIMA Katsushige

*Senior Researcher, EMC Measurement Group, Wireless Communications Department
EMC Measurement*



SUGIYAMA Tsutomu

*Researcher, EMC Measurement Group, Wireless Communications Department
EMC Measurement*



YAMANAKA Yukio

*Group Leader, EMC Measurement Group, Wireless Communications Department
EMC Measurement*



SHINOZUKA Takashi

*Research Supervisor, Wireless Communications Department
Electromagnetic Compatibility*